

# A Comprehensive Correlation between Lattice Strain and Quantum Well Thickness of MBE Grown AlGaAs/InGaAs/GaAs Pseudomorphic HEMT with Device Performance for Transconductance and Linearity

Partha Mukhopadhyay<sup>1</sup> (Member, IEEE), Palash Das<sup>1</sup>, Saptarshi Pathak<sup>1</sup>, Edward Y. Chang<sup>2</sup> (Senior Member, IEEE) and Dhruves Biswas<sup>1</sup> (Senior Member, IEEE)

<sup>1</sup>Department of Electronics and Electrical Communication Engineering, Indian Institute of Technology – Kharagpur, India

<sup>2</sup>Department of Material Science and Engineering, National Chiao Tung University, Hsinchu, Taiwan

[partha@ece.iitkgp.ernet.in](mailto:partha@ece.iitkgp.ernet.in), Ph: +91-9434502268

**KEYWORDS:** PHEMT, lattice mismatch, critical thickness, mobility, sheet concentration,  $g_m$

## Abstract

**Molecular Beam Epitaxy (MBE) grown quantum well (QW) based InGaAs/AlGaAs/GaAs modulation doped heterostructure devices have been studied as an insight to epitaxial growth physics. Analysis of the pre-process characterization data reveals the strain in structure with respect to the varying QW thickness and extends to the bandgap energy discrepancy. Detailed physics based explanation has been presented for mobility and carrier concentration variations in terms of crystallographic aspects. The post-process device data through ATLAS, SILVACO simulation for output saturation current ( $I_D$ ), and transconductance ( $g_m$ ) correlation has been analyzed for prediction of the impact on device performances.**

## INTRODUCTION

Indium Gallium Arsenide channel based high electron mobility transistor (HEMT) has become the device of choice for high performance applications [1]. Advanced carrier transport and other favorable electronic properties of compound semiconductor heterostructure based InGaAs/GaAs High Electron Mobility Transistor (HEMT) has the capability to achieve low cost high speed devices at moderately high operating frequency range with superior linearity. The prime motivation behind this study of the crystal lattice strain with quantum well thickness in terms of InGaAs channel layer is to produce dislocation free coherent high quality crystal growth.

The PHEMT epitaxial layer structures were grown by Molecular Beam Epitaxy reactor at our IIT Kharagpur lab. All the epitaxial structures were unique in terms of composition except the thickness of the channel. It varied between 6.5nm to 13nm in different samples. Characterization and process of the samples were done at Solid State Physics Laboratory (SSPL), Delhi, India. ATLAS SILVACO simulation was used to simulate the devices by solving Poission's Equation and Schrodinger Equation for realization of further device optimization.

## GROWTH OF THE DEVICE STRUCTURE

The studied PHEMT devices, shown in Fig. 1, were grown on a 2<sup>0</sup>-cut off-axis (100) SI-GaAs wafer from Sumitomo. The samples were grown by epitaxial C-12 MBE reactor at our HPDG (High Performance Device Group) lab, IIT Kharagpur, India. The epitaxial structure consists of a buffer, active layer, spacer, barrier, and cap layer. The 350nm undoped GaAs buffer was grown at 580<sup>0</sup>C growth temperature. Undoped In<sub>x</sub>Ga<sub>1-x</sub>As channel layer with indium mole fraction of 0.17 was grown at relatively lower temperature. Three samples had varying channel thicknesses of 6.5nm, 10.5nm and 13nm. Relatively high bandgap of the lower indium mole of InGaAs channel (1.18eV) limits impact ionization effects and the high band gap of the AlGaAs Schottky layer (1.75eV) improves the turn-on voltage [2], which results in a better on-state Breakdown Voltage (BV), a main limiting factor for power devices [3, 4]. A thin (5 Å) undoped Al<sub>0.26</sub>Ga<sub>0.74</sub>As spacer layer was sandwiched between the channel and the barrier. The 40 nm thick Al<sub>0.26</sub>Ga<sub>0.74</sub>As layer was doped with Si with average doping concentration of 5x10<sup>17</sup>cm<sup>-3</sup>. Finally, the Si doped 80 Å GaAs cap layer was grown on top of the PHEMT structure. The growth was commented with nice and bright in-situ 2x4 RHEED reconstruction observations in Arsenic rich condition.

<b>Doped 5E17 GaAs cap Layer t=0.008μ</b>
<b>Doped 5E17, AlGaAs, Al=26% t=.04 μ</b>
<b>AlGaAs, Al=26% t=0.005 μ</b>
<b>InGaAs, In=17% t = 6.5/10.5/13nm for M0010/M0009/M0008</b>
<b>SI-GaAs (Substrate)</b>

Fig 1: In<sub>0.17</sub>Ga<sub>0.83</sub>As/AlGaAs PHEMT

## RESULT AND DISCUSSION

Considering the Matthews and Blakeslee model [5] we have designed the pseudomorphic AlGaAs/InGaAs structures with Indium mole fraction as in Fig. 1 with varying channel thicknesses between 65Å to 130Å and found that 105Å is an optimized structure. We have calculated the compressive force ( $F_c$ ) and tensile force ( $F_t$ ), in GPa unit, generated on the channel. Fig. 2 shows the variation of  $F_c$  and  $F_t$  of the samples with respect to the channel thickness. Analyzing the plot it can be seen that from 13nm samples compressive force is starting surpluses to the tensile force but as  $F_c < 2F_t$  the interface and the channel stands as coherent.

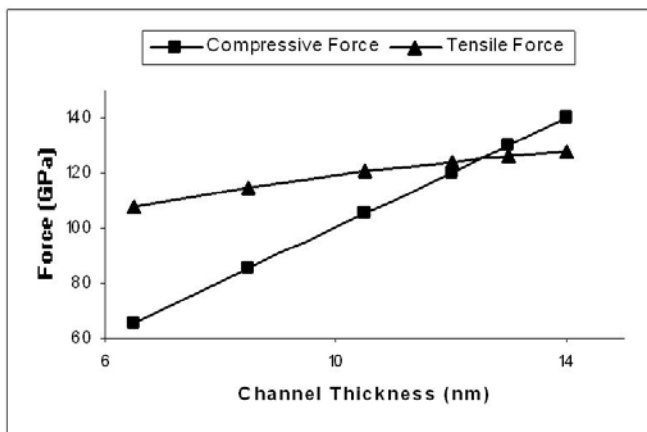


Fig 2: Variation of  $F_c$  and  $F_t$  with channel thickness

We kept the growth parameters in such a way that every component of all the structures were unique except the channel thickness, which reflects in XRD results as shown in Fig. 3(a). In other words the lattice constant fraction was same, i.e. effective mass was same, only QW thickness varied which resulted a change in the strain component and hence the bandgap. The photoluminescence data of the 3 samples are shown in Fig. 3(b). Narrowing the channel thickness sharpens the InGaAs/AlGaAs heterojunction and as a result AlGaAs peak is more prominent in thinner channels. The blue shift of the peaks with decreasing channel thickness explains the increasing effective bandgap of the QW. It can also be correlated with the experimental results shown in Fig. 2. The higher compressive strain in thicker channel samples, results into split-off of heavy-hole and light-hole at valance band and the consequence is the decreasing effective bandgap. It is well depicted in Fig. 4 and can easily be verified. The bandgap has drastically decreased in wider channels also because the additional quantum levels in QW lower the effective conduction band minima. This actually results in confinement of more electrons in QW and increase in mobility as shown in Fig. 5. In case of sample M0010 the mobility is less as scattering dominates in narrow channel which has less effective sheet

concentration too. M0009 sample has best mobility whereas M0008 has less mobility due to the dominant factor of compressive strain, as shown in Fig. 2, hence misfit dislocations at heterointerface.

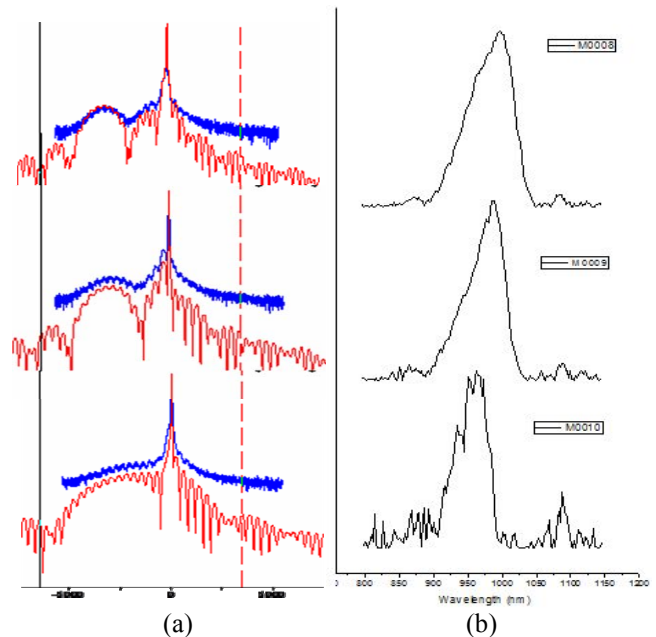


Fig 3: (a) XRD pattern with simulation pattern (b) PL spectra of sample M0008, 9 & 10 (from top) with channel thickness of 13nm, 10.5nm & 6.5nm respectively. Philips X-pert MRD HRXRD system was used to characterize the epitaxial layer of the all samples.

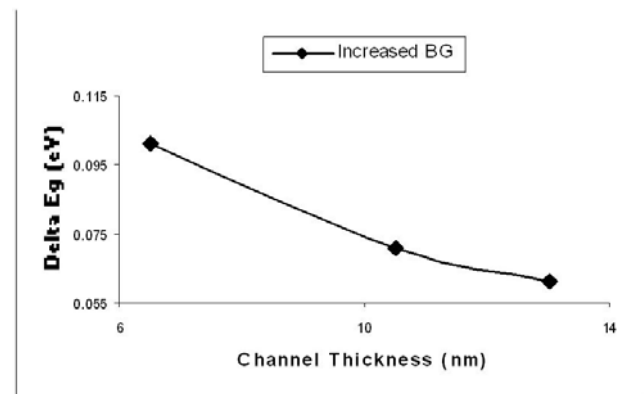


Fig 4: Variation of difference of QW bandgap and bulk channel bandgap with channel thickness

For post process DC characteristics data of the same samples reveals that M0009 sample with 10.5nm channel thickness has optimized results than other. The output saturation current  $I_D$  @1.6 V of the 10.5nm channel thickness sample is almost 55% higher than 6.5nm sample and around 7.5% higher than 13nm sample. The variation of saturation current again solidifies the conception we have discussed previously regarding the decrease in effective bandgap with increasing the channel thickness. This deviation might be the cause of increase in effective conduction band discontinuity  $\Delta E_c$  [6]. It means that decreased alloy scattering and increased 2DEG

concentration will result in wider channel; which will increase the drain current and consequently  $g_m$ .

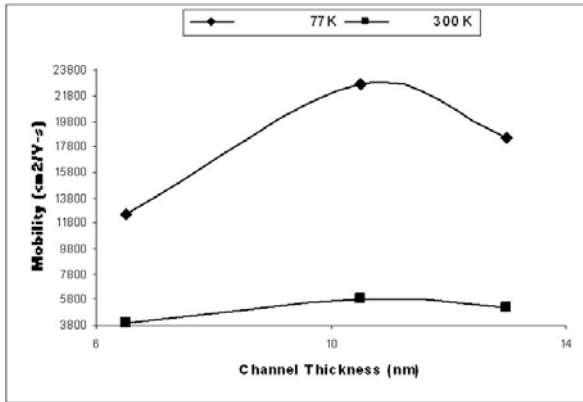


Fig 5: Mobility (both 77K and 300K) with channel thickness

We have also simulated the same structures using ATLAS, SILVACO with gate length of  $0.1\mu\text{m}$  and found almost similar type of information. Saturation output current of the samples is  $322\text{mA/mm}$ ,  $329\text{mA/mm}$  and  $332\text{mA/mm}$  of M0010, M0009 and M0009 respectively. One prototype plot of output drain current of M0008 sample is shown in Fig. 6.

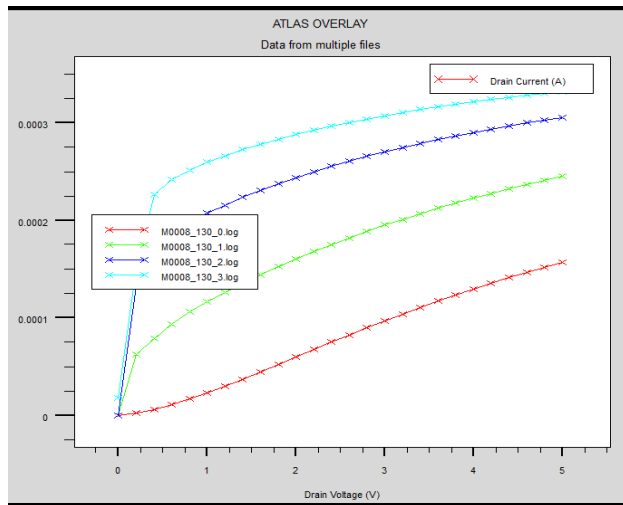


Fig 6: Drain current of M0008 PHEMT sample

Variation of saturation current and  $g_m$  are plotted with respect to different channel length and shown in the Fig 7. As per simulation results concerned with the M0009 sample, it has higher  $I_D$  and  $g_m$  value than M0010 and is comparable with M0008 sample. Variation of  $I_D$  in case of simulation result is little different than the actual process data which may be the result of the limitation of the simulator for our experimental condition due to insufficient consideration of some model parameters regarding stress/strain generated at the heterointerface during epitaxial growth of different materials. A narrow channel would give a smaller gate-to-2DEG separation, as well as higher aspect ratio for better control of the gate potential over the charge carriers. Therefore,  $g_m$  seems to be high in narrow channel HEMT in

terms of better gate potential control on 2DEG. Hence, the two competing factors leads to the variation of  $g_m$ , eventually reduces the variation of the  $g_m$  value among the samples.

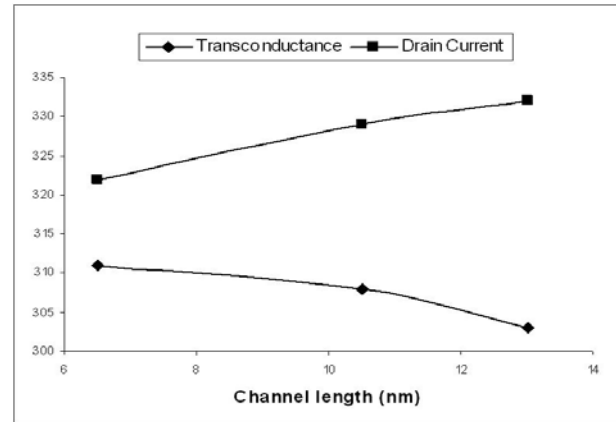


Fig 7: Variation of  $I_D$  and  $g_m$  of M0008, M0009 & M0010 PHEMT Sample

## CONCLUSIONS

In this paper we have grown several InGaAs/AlGaAs/GaAs PHEMTs by MBE in our lab. The three referenced grown structures have different channel thicknesses of 6.5nm, 10.5nm and 13nm respectively. Analyzing the PL spectra, XRD and Hall data we have found that the sample with 10.5nm channel thickness is an optimized structure. Post process data and ATLAS (SILVACO) simulation of the samples for DC characteristics correlate the property based analysis with  $I_D$  and  $g_m$  performances. Analyzing the  $g_m$  curve and IP3 which is proportional to  $(g_m''/g_m)$ , the ratio of third-order sideband power to fundamental power [4], it can be said that the devices can be best useful as low noise applications. Though the sheet concentration is very close to  $2e12\text{ cm}^{-2}$  but saturation current is limited by the lower doping in cap layer.

Our future work is lying in integration of III-V compound semiconductor on matured Si technology using metamorphic technique by sophisticated epitaxial growth process keeping in view of such physics based correlation.

## ACKNOWLEDGEMENT

We are very thankful to DIT, Govt. of India for funding the research work under the project No. 20(3)/2007-NANO. For support in characterization and process of the samples we are very thankful to SSPL, Delhi. Our sincere gratitude goes to Advanced VLSI Lab, IIT Kharagpur for providing simulation software support.

## REFERENCES

- [1] P. Mukhopadhyay, D. Biswas et al; IEEE-NANO-2008, USA
- [2] Zaknourne, M. et al., IEEE EDL, pp, 345-347, vol 19, no 9, Sept 1998
- [3] P. Mukhopadhyay, D. Biswas et al; IEEE-NANO-2009, Italy
- [4] P. Mukhopadhyay, D. Biswas et al; CSMANTECH 2010, USA
- [5] J.W. Matthews & A.E. Blakeslee, J. Cryst Grwth 32 (1976) 265
- [6] S.R. Bahl, J.A. del Alamo; IEEE Electron. Dev. Lett. 13 (1992)